CHALMERS
UNIVERSITY OF TECHNOLOGY

Wideband mm-wave Spectrum-Efficient Transmitter Using Low-Pass Sigma–Delta-Over-Fiber Architecture

Citation for the original published paper (version of record):
Bao, H., Ponzini, F., Fager, C. (2023). Wideband mm-wave Spectrum-Efficient Transmitter Using Low-Pass Sigma–Delta-Over-Fiber
Architecture. IEEE Microwave and Wireless Technology Letters, 33(10): 1505-1508.
http://dx.doi.org/10.1109/LMWT.2023.3304479

(article starts on next page)

Wideband mm-wave Spectrum Efficient Transmitter Using Lowpass Sigma-Delta-over-Fiber Architecture

Husileng Bao, *Student Member, IEEE*, Filippo Ponzini, and Christian Fager, *Senior Member, IEEE*

***Abstract*—The millimeter-wave band offers large bandwidth and promises high data rates for wireless communication systems. This work proposes a millimeter-wave radio-over-fiber architecture suitable for wideband mm-wave communication, using a lowpass sigma-delta modulation approach. The central unit generates baseband sigma-delta bitstreams, in-phase/quadrature (I/Q) components, which are transported to a remote radio head (RRH) using a standard QSFP28 optical interconnect link connection. In the RRH, the baseband I/Q signals are upconverted to the millimeter-wave band, amplified, and transmitted through an antenna. The performance of the resulting sigma-delta-over-fiber transmitter architecture is experimentally verified at 28 GHz, demonstrating a state-of-the-art symbol rate up to 1.5 Gsym/s. Furthermore, in over-the-air measurements, the architecture is shown to support 1 Gsym/s with 5.9% error vector magnitude for 64/256/1024 quadrature amplitude modulation cases over a 5 m wireless distance. The results demonstrate the feasibility of the proposed architecture for the realization of wideband millimeter-wave distributed antenna systems.**

***Index Terms*– Sigma-delta-over-fiber, over-the-air, millimeter-wave.**

I. Introduction

Wireless communication networks require high data rates to support an ever increasing amount of user subscriptions and data traffic volumes [1] [2]. Millimeter-wave (mm-wave) frequency has wider available bandwidth and increases data rates. Radio-over-fiber (RoF) is a key and mature technology for low-frequency (sub-6 GHz) communication systems [3], and also suitable for distributed antenna systems which is one direction to increase communication capacity [4]. Nevertheless, in any area, the available bandwidth is limited for a specific wireless system [5], therefore promoting solutions for increased spectrum efficiency rather than bandwidth. The first option for increased spectral efficiency is to explore spatial diversity as in multiple-input-multiple-output (MIMO) systems [6]. The second solutions use high modulation order to increase spectral efficiency. Hence, to keep up with the demands, there is a need for mm-wave MIMO systems supporting high modulation order.

Several wideband mm-wave analog RoF (ARoF) transmitters have been implemented with laboratory equipments [7]–[16], as reported in TABLE I. However, none of them supports spectrally efficient MIMO operation, and with only low efficient modulation schemes of on-off-keying (OOK)/quaternary-amplitude-shift-keying (4ASK)/quadrature phase shift keying (QPSK)/16QAM/32QAM (quadrature amplitude modulation).

Manuscript received xxxxxxx xx, 2023; revised xxxxxxx xx, 2023; accepted xxxxxxx xx, 2023. This work has received funding from the European Union's Horizon 2020 research and innovation programme under the Marie Skłodowska-Curie grant agreement No 860023. (Corresponding author: Husileng Bao.)

Husileng Bao and Christian Fager are with the Department of Microtechnology and Nanoscience, Chalmers University of Technology, SE-412 96 Gothenburg, Sweden (e-mail: husileng@chalmers.se; christian.fager@chalmers.se).

Filippo Ponzini is with the GFTL ER HDE Optical Systems, Ericsson Research, IT-561 24 Pisa, Italy (e-mail: filippo.ponzini@ericsson.com).

TABLE I
STATE-OF-THE-ART RADIO-OVER-FIBER TRANSMITTERS.

Ref.	Carrier (GHz)	Modulation	Capacity (Gsym/s)	EVM (%)	Complexity
[7]	159.6	OOK	12.5	-	High
[8]	37.75	4ASK	-	-	High
[9]	28	QPSK	0.1	8	High
[10]	28	16QAM	1.96	-	High
[11]	28	16QAM	-	10	High
[12]	28.4	16QAM	-	4.18	High
[13]	60	16QAM	1.76	-	High
[14]	19	16QAM	3	15.25	High
[15]	141	16QAM	44	-	High
[16]	60	32QAM	0.1	7.9	High
[17]	28	64QAM	2.2	7.6	High
[18]	28.25	64QAM	0.1	-	High
[19]	28	64QAM	0.8	-	Medium
[20]	>24	64QAM	0.16	7.11	Medium
[21]	123	4096QAM	15	-	High
[22]	76.2	8192QAM	10	-	High
This work	28	1024QAM	1	5.9	Low

The systems in [17] [18] used 64QAM signals with a Mach-Zehnder modulator (MZM) and an external laser source to modulate the radio frequency (RF) signal to the optical domain, which results in high system complexity. The MIMO demonstration of [19] is based on an intermediate-frequency-over-fiber (IFoF) architecture with off-the-shelf hardware. A bandpass sigma-delta-over-fiber (SDoF) MIMO architecture is reported in [20] with medium complexity, but the results were limited by the 10 Gbps data rate of the fiber connection and phase noise of the radio. Recently, the mm-wave demonstrations of [21] [22] showed 4096/8192QAM modulated signals, respectively, with highly complex arbitrary waveform generator (AWG) and external laser equipments in the central unit (CU). The demodulated results of [21] [22] depended on a 25% overhead forward error correction (FEC) and did not report any EVM.

In our previous research, we introduced a new bandpass SDoF based mm-wave MIMO link architecture [23]. In [24], we performed detailed investigations on the architecture and presented MU-MIMO transmission, serving two users with 500 Msym/s each using 64QAM modulation.

In this work, we propose a baseband/low-pass sigma-delta approach to extend the bandwidth and signal spectrum efficiency for mm-wave SDoF architectures. Additionally, this work has an even simpler remote radio head (RRH) solution than in [24]. We report state-of-the-art performance with 5 m OTA transmission of 28 GHz 64/256/1024QAM modulated signals with $\geq$4 Gbit/s throughput.

This paper is structured as follows: Section II describes the system architecture. Section III presents the results of the experimental investigations. Finally, conclusions are drawn in Section IV.

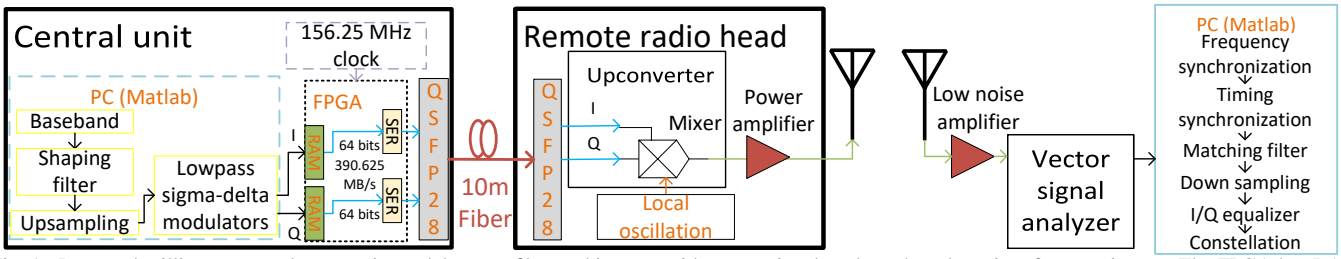

Fig. 1. Proposed millimeter-wave lowpass sigma-delta-over-fiber architecture with vector signal analyzer based receiver for experiments. The FPGA has RAM (random access memory) and SER (serializer) for data transmission at 25 Gbps = 64 bits×4390.625 MB/s.

II. System Architecture

The proposed architecture is reported in Fig. 1. In the CU, the baseband signal is upsampled to a data rate of 25 Gsym/s and then fed to two second-order lowpass sigma-delta modulators (LP-SDM) for the I and Q components, respectively. A FPGA (Virtex UltraScale+ HBM VCU128) with a 156.25 MHz clock rate and a QSFP28-enabled fiber connection transmit LP-SDM bitstreams from the CU to the RRH. QSFP28 (FS QSFP-100G-SR4-S) is a standardized optical interconnection with four parallel channels, each operating at 25 Gbps. The fiber connection is a 10m MTP-12 (female) to MTP-12 (female) cable with twelve OM4 multimode fibers. Only two sub-channels of fiber connection are operating to study the LP SDoF principle in this work. All four sub-channels of the QSFP28 will be occupied in future MIMO extensions. In the future, the capacity of our proposed system can scale up significantly since 800 Gbps pulse amplitude modulation 4-level (PAM4) fiber link solutions are available.

The RRH contains a mm-wave upconverting mixer (Analog Devices EVAL-ADMV1013), which has an output frequency range of 24-44 GHz. In this case, the mixer is configured for baseband operating mode and requires a local oscillator (LO) signal of 5.4-10.25 GHz due to its built-in LO quadrupler. During measurements, a 7 GHz LO frequency is used, corresponding to a 28 GHz output frequency. The mixer also has integrated LP filters for input baseband signals with a 6 GHz cut-off frequency, suppressing part of the quantization noise in the LP-SDM coded I/Q signals. In a real application, a separate LP filter will be installed, matching the symbol rate used. Connected to the mixer is a 24 - 34 GHz power amplifier (Analog Devices EVAL-HMC943APM5E), which boosts the transmitter output power and the OTA range.

The RRH is equipped with a Vivaldi antenna designed for a 28 GHz center frequency. An identical antenna is used at the receiver in the OTA experiments. where a low noise amplifier is connected before a 33 GHz oscilloscope (UXR0334A Infiniium UXR-Series, 128 GS/s) equipped with a vector signal analyzer (VSA) software. The receiver signal processing compensates for I/Q imbalance using a 25 taps I/Q equalizer.

III. Experimental Results

The experiments with the proposed transmitter have been done with the setup illustrated in Fig. 2. In the following, we present a stage-by-stage verification of the RRH, and OTA experiments.

A. RRH Verification

The performance of the RRH has been investigated in terms of its power, spectrum, and symbol rate. In the RRH, LP-SDM coded I/Q signals from the QSFP28 transceiver are fed to the active mixer, which has a programmable gain amplifier at its output stage. When we change the mixer output power from -15.8 dBm to 6.5 dBm, the EVM of the output signal worsens as Fig. 3 shows. The measured power is the band power for the 100 Msym/s 64-QAM modulated signal, which has around 6 dB peak-to-average-power-ratio. It means that the mixer, with an output 1 dB compression point of 10 dBm, introduces a distortion to the high power output signal.

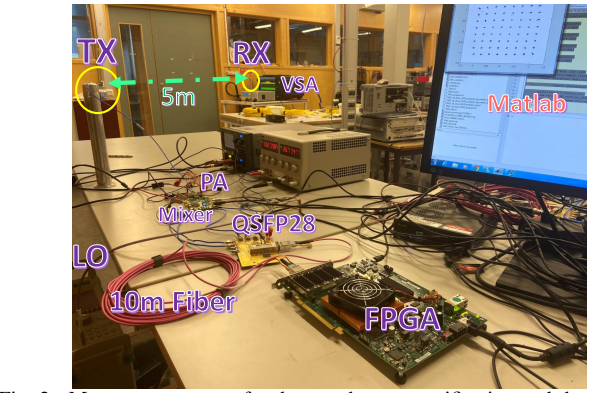

Fig. 2. Measurement setup for the step-by-step verification and the over-the-air demonstration.

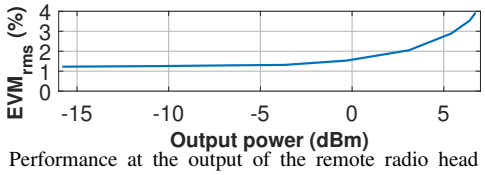

Fig. 3. Performance at the output of the remote radio head upconverting mixer.

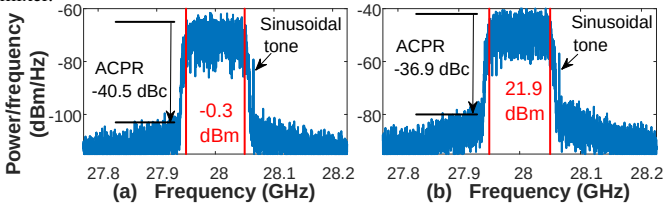

Fig. 4. In-band power and adjacent channel power ratio (ACPR) at the output of (a) Upconversion mixer; (b) Power amplifier. A sinusoidal tone is added to track the carrier frequency offset.

To have enough power for OTA transmission, we configured the output power of the mixer to -0.3 dBm, as illustrated by the spectrum in Fig. 4(a). On the right side of the inband signal, a sinusoidal tone is added to track carrier frequency offset between the transmitter and the receiver since they are not synchronized. The adjacent channel power ratio (ACPR) is -40.5 dBc at the mixer output for the 100 Msym/s 64-QAM single carrier transmission case. At the output of the PA, the signal power is increased to 21.9 dBm as Fig. 4(b) presents, which corresponds to a 22.2 dB = 21.9 dBm - (-0.3 dBm) gain. This corresponds well to the PA data sheet, where a

20 dB minimum gain is specified. From the results in Fig. 4, the ACPR degrades from -40.5 to -36.9 dBc after the PA. The reason is that the output signal power is close to the 1 dB compression point of the PA, which is 29 dBm. The peak output power reaches 28.6 dBm when considering the 6.7 dB peak-to-average power of the signal used. The LP-SDM quantization noise is potentially contributing to additional power.

To visualize the quantization noise of the SDM signal, Fig. 5(a) shows the measured spectrum of the QSFP28 output signal and shows that the quantization noise extends up to 20 GHz, while the spectrum of Fig. 5(b) proves that a LP filter with 200 MHz can suppress the noise at least 35 dB. However, the following measurements do not include such a LP filter since our objective is to investigate symbol rate limitations of the proposed architecture.

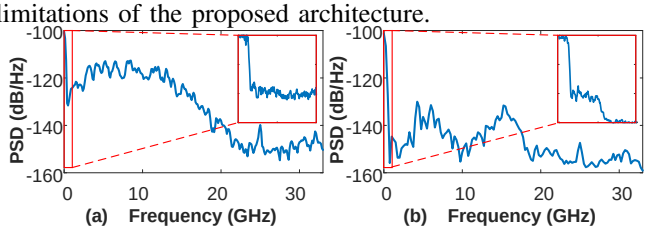

Fig. 5. Spectrum of (a) the QSFP28's signal; (b) the QSFP28's signal with a lowpass filter.

Fig 6 shows the wideband spectrum of the mm-wave output signal. Even if the transmitting signal is at least 20 dB higher than the quantization noise, the quantization noise is present across the entire band from 20-33 GHz, which is the upper limit of the instrument used. Hence, it is reasonable that the quantization noise contributes some power.

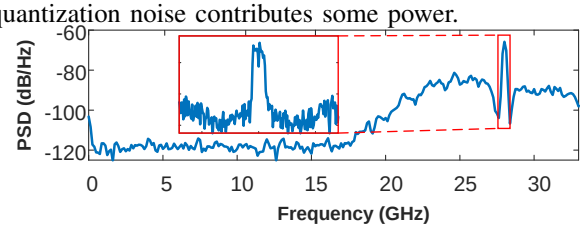

Fig. 6. Spectrum of the remote radio head output signal.

The symbol rate performance is measured at the QSFP28/mixer/PA outputs, respectively, and compared with simulation results as reported in Fig. 7. For the QSFP28 output signal, two channels of the oscilloscope (33 GHz bandwidth) sample the I and Q data simultaneously. For the mixer and PA signal, one channel of the oscilloscope samples the mm-wave signal in VSA mode. In general, the quality of the QSFP28 signal, quantified by its EVM, is close to the performance after upconversion in the mixer, with a small degradation due to the chosen nonlinearity output power tradeoff discussed previously. At 1.5 Gsym/s, all measured results are close to the theoretical limit set by the quantization noise from the SDM sample rate. It means that the SDM signal quantization distortion dominates the transmitter performance.

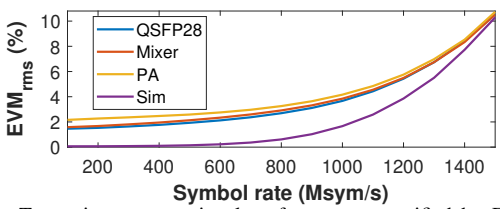

Fig. 7. Transmitter output signal performance quantified by EVM for 64-QAM modulated signal up to 1.5 Gsym/s.

B. OTA Experiments

During the OTA experiments, the transmit antenna is separated from the receive antenna by a 5 m distance, as Fig. 2 shows. The OTA experiments have three modulation cases: 64/256/1024QAM. As shown in the results in Fig. 8(a), the EVM is independent of the modulation order used, demonstrating an EVM around 8% at 1 Gsym/s. The difference between the OTA curves and the results directly at the RRH PA output is caused by the received signal power spectral density decreasing in proportion to the bandwidth increases. A shorter distance, higher output power, or more directive antennas could recover this.

The bit-error without FEC is calculated because it is a stricter requirement than the EVM. The zero-error symbol rates for 64/256/1024QAM signals are 800/500/200 Msym/s, obtained from ten transmissions of 46080/38400/19200 bits. Fig. 8(b) presents the corresponding demodulated constellations of 800/500 Msym/s 64/256QAM signals with 6.1%/3.8% EVM corresponding to 4.8 Gbit/s and 4 Gbit/s. In general, the lower modulation formats reach a larger data rate, while the higher modulation formats promise higher spectrum efficiency.

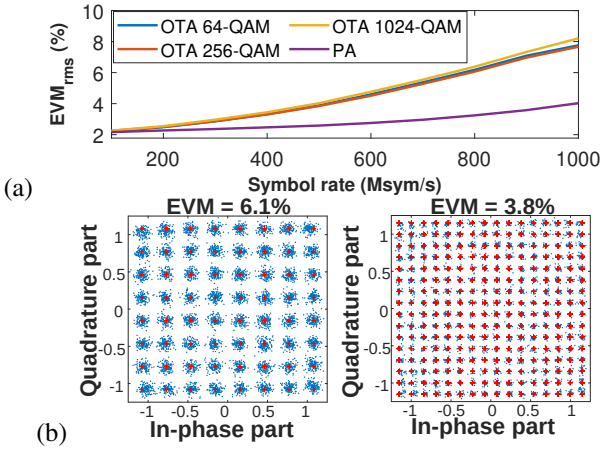

Fig. 8. Results of the over-the-air measurements. (a) Error vector magnitude (EVM) performance; (b) Zero-error constellations for 64/256 quadrature amplitude modulation.

IV. Conclusion

This paper proposes a mm-wave transmitter architecture using QSFP28-enabled lowpass SDoF with a low-cost hardware implementation. The lowpass SDM allows larger bandwidth than the typical bandpass SDoF implementations. The transmitter verification reaches a symbol rate of 1.5 Gsym/s with 10.7% EVM, while 1 Gsym/s still has 4.2% EVM. Moreover, the OTA measurements operate at 28 GHz carrier frequency over a 5 m distance, resulting in 8% EVM for spectrally efficient 64/256/1024QAM signals, with the zero-error data rates of 4.8 Gbit/s and 4 Gbit/s for 64/256QAM signals. The results demonstrate the feasibility of the proposed architecture for the realization of wideband mm-wave distributed antenna systems.

Acknowledgment

The authors want to thank Xilinx for the donation of the Virtex UltraScale+ HBM VCU128 FPGA Evaluation Kit and the license to the Vivado software. The authors also want to thank Analog Devices for the donation of the EVAL-HMC943APM5E evaluation board for this work.

REFERENCES

[1] Cisco, "Cisco Annual Internet Report," 2023. [Online]. Available: https://www.cisco.com/c/en/us/solutions/executive-perspectives/annual-internet-report/index.html

[2] Ericsson, "Ericsson Mobility Report," 2022. [Online]. Available: https://www.ericsson.com/en/reports-and-papers/mobility-report/mobility-visualizer

[3] C. Lim, Y. Tian *et al.*, "Evolution of radio-over-fiber technology," *Journal of Lightwave Technology*, vol. 37, no. 6, pp. 1647–1656, 2019.

[4] Ö. T. Demir, E. Björnson, and L. Sanguinetti, "Foundations of user-centric cell-free massive MIMO," *Foundations and Trends® in Signal Processing*, vol. 14, no. 3-4, pp. 162–472, 2021.

[5] L. Boucher, "Frequency allocations and regulations in the 50-to-70-GHz band," in *2000 Asia-Pacific Microwave Conference. Proceedings (Cat. No.00TH8522)*, 2000, pp. 116–119.

[6] E. G. Larsson, O. Edfors *et al.*, "Massive MIMO for next generation wireless systems," *IEEE Communications Magazine*, vol. 52, no. 2, pp. 186–195, 2014.

[7] R. Maximidis, C. Vagionas *et al.*, "Demonstration of Low-Complexity D-band Extension of Fiber X-haul for 5G and Beyond Infrastructure," in *2023 17th European Conference on Antennas and Propagation (EuCAP)*, March 2023, pp. 1–4.

[8] A. H. M. R. Islam, M. Bakaul, and A. Nirmalathas, "Multilevel Modulations for Gigabit Access in a Simple Millimeter-Wave Radio-Over-Fiber Link," *IEEE Photonics Technology Letters*, vol. 24, no. 20, pp. 1860–1863, 2012.

[9] N. Tawa, T. Kuwabara *et al.*, "28 GHz over-the-air measurement using an OTFS multi-user distributed MIMO under Doppler effect," *International Journal of Microwave and Wireless Technologies*, p. 1–8, 2023.

[10] D. Konstantinou, T. A. Bressner *et al.*, "5G RAN architecture based on analog radio-over-fiber fronthaul over UDWDM-PON and phased array fed reflector antennas," *Optics Communications*, vol. 454, p. 124464, 2020.

[11] L. Bogaert, J. Van Kerrebrouck *et al.*, "SiPhotonics/GaAs 28-GHz Transceiver With Reflective EAM for Laser-Less mmWave-Over-Fiber," *Journal of Lightwave Technology*, vol. 39, no. 3, pp. 779–786, 2021.

[12] R. Budé, M. M. Versluis *et al.*, "Millimeter-Wave Outphasing using Analog-Radio over Fiber for 5G Physical Layer Infrastructure," in *2020 50th European Microwave Conference (EuMC)*, 2021, pp. 288–291.

[13] T. Nagayama, S. Akiba *et al.*, "Photonics-Based Millimeter-Wave Band Remote Beamforming of Array-Antenna Integrated With Photodiode Using Variable Optical Delay Line and Attenuator," *Journal of Lightwave Technology*, vol. 36, no. 19, pp. 4416–4422, 2018.

[14] M. Morant, A. Trinidad *et al.*, "Multi-Beamforming Provided by Dual-Wavelength True Time Delay PIC and Multicore Fiber," *Journal of Lightwave Technology*, vol. 38, no. 19, pp. 5311–5317, 2020.

[15] R. Puerta, J. Yu *et al.*, "Single-Carrier Dual-Polarization 328-Gb/s Wireless Transmission in a D-Band Millimeter Wave 2 × 2 MU-MIMO Radio-Over-Fiber System," *Journal of Lightwave Technology*, vol. 36, no. 2, pp. 587–593, 2018.

[16] C. Vagionas, E. Ruggeri *et al.*, "Linearity Measurements on a 5G mmWave Fiber Wireless IFoF Fronthaul Link With Analog RF Beamforming and 120° Degrees Steering," *IEEE Communications Letters*, vol. 24, no. 12, pp. 2839–2843, Dec 2020.

[17] I. Lima de Paula, L. Bogaert *et al.*, "Air-Filled SIW Remote Antenna Unit With True Time Delay Optical Beamforming for mmWave-Over-Fiber Systems," *Journal of Lightwave Technology*, vol. 40, no. 20, pp. 6961–6975, 2022.

[18] K. Ito, M. Suga *et al.*, "Passive beamformer based remote beamforming scheme for radio-over-fiber systems: Experimental demonstration using 28-GHz band reflectarray," *Optics Communications*, vol. 513, p. 128026, 2022.

[19] M. Sung, J. Kim *et al.*, "Demonstration of 5G Trial Service in 28 GHz Millimeter Wave using IFoF-Based Analog Distributed Antenna System," in *2019 Optical Fiber Communications Conference and Exhibition (OFC)*, 2019, pp. 1–3.

[20] C.-Y. Wu, H. Li *et al.*, "Distributed Antenna System Using Sigma-Delta Intermediate-Frequency-Over-Fiber for Frequency Bands Above 24 GHz," *Journal of Lightwave Technology*, vol. 38, no. 10, pp. 2765–2773, 2020.

[21] W. Li, Y. Wang *et al.*, "Delivery of 103.2 Gb/s 4096QAM signal over 180m wireless distance at D-band Enabled by Truncated Probabilistic Shaping and MIMO Volterra Compensation," in *Optical Fiber Communication Conference (OFC) 2022*. Optica Publishing Group, 2022, p. M1C.4.

[22] Z. Ju, J. Liu, and J. Yu, "W-band radio-over-fiber transmission system with delta-sigma modulation and direct detection," *Chin. Opt. Lett.*, vol. 21, no. 4, p. 040602, Apr 2023.

[23] H. Bao, Z. S. He *et al.*, "Demonstration of Flexible mmWave Digital Beamforming Transmitter using Sigma-Delta Radio-Over-Fiber Link," in *2022 52nd European Microwave Conference (EuMC)*, 2022, pp. 692–695.

[24] H. Bao, F. Ponzini, and C. Fager, "Flexible mm-Wave Sigma-Delta-Over-Fiber MIMO Link," *Journal of Lightwave Technology*, vol. 41, no. 14, pp. 4734–4742, July 2023.